Erythrocyte hemodynamics in stenotic microvessels: A numerical investigation

T. Wang[1,*] and Z. W. Xing[2,†]

[1]*Department of Mathematics, Nanjing University of Aeronautics and Astronautics, Nanjing 210016, China*

[2]*Department of Materials Science and Engineering, Nanjing University, Nanjing 210093, China*

(Received 12 December 2012; revised manuscript received 3 October 2013; published 29 October 2013)

This paper presents a two-dimensional numerical investigation of deformation and motion of erythrocytes in stenotic microvessels using the immersed boundary-fictitious domain method. The erythrocytes were modeled as biconcave-shaped closed membranes filled with cytoplasm. We studied the biophysical characteristics of human erythrocytes traversing constricted microchannels with the narrowest cross-sectional diameter as small as 3 μm. The effects of essential parameters, namely, stenosis severity, shape of the erythrocytes, and erythrocyte membrane stiffness, were simulated and analyzed in this study. Moreover, simulations were performed to discuss conditions associated with the shape transitions of the cells along with the relative effects of radial position and initial orientation of erythrocytes, membrane stiffness, and plasma environments. The simulation results were compared with existing experiment findings whenever possible, and the physical insights obtained were discussed. The proposed model successfully simulated rheological behaviors of erythrocytes in microscale flow and thus is applicable to a large class of problems involving fluid flow with complex geometry and fluid-cell interactions. Our study would be helpful for further understanding of pathology of malaria and some other blood disorders.

DOI: 10.1103/PhysRevE.88.042711 PACS number(s): 87.85.gf, 47.63.Cb, 87.16.dm

I. INTRODUCTION

Human erythrocyte, also known as red blood cell, is a membrane envelope filled with cytoplasm and supported by a cytoskeletal structure. The cytoplasm of erythrocytes behaves as a Newtonian fluid with viscosity five times that of the blood plasma. The cytoskeleton is a two-dimensional network which is very flexible and compressible. The fluidity of the human erythrocytes is due to the cytoskeletal structure of their membrane [1,2]. The cells can rearrange components of their cytoskeleton, allowing the cells to become almost liquidlike. In fact, cytoskeletal changes can result in changes in the overall mechanical properties of the cell and in their cellular functions.

In static blood plasma and large blood vessels, healthy erythrocytes present as biconcave-shaped disks with diameter about 8 μm and thickness about 2 μm. However, during their 120-day life span, they are forced to repeatedly squeeze through microvessels of smaller size than themselves. So the cells must undergo severe deformation to fit in and to reduce flow resistance. In addition, large deformation can also occur in capillaries and arterioles where erythrocytes do not travel in isolation and their interactions with one another and the vascular wall cause them to stretch. They usually deform into parachute shapes, slipper shapes [3,4], or even bullet shapes [5] in order to fit in microvessels. This kind of deformation will not produce permanent damage to the cell because the cell membrane is flexible enough to recover the biconcave shape whenever the force on the cell is released. On the other hand, the deformability of erythrocytes significantly affects the flow behavior in the microcirculation [6].

Human diseases, such as malaria, cancer, and sickle cell anemia, can cause not only changes in the shape of the erythrocytes, but also variations in mechanical properties of erythrocyte membrane, usually change of deformability and/or adhesion strength. For instance, hereditary elliptocytosis and hereditary spherocytosis are both cell membrane disorders in which the erythrocytes become elliptical or spherical and suffer with membrane loss, decreased surface area, and decreased deformability. The malaria infected erythrocytes become more rigid (could be more than ten times than healthy cells) and adhesive in comparison with healthy ones [7,8], which may significantly affect normal blood circulation and lead to capillary occlusions [9]. As a result, malaria patients become severely anemic and suffer from symptoms related to insufficient oxygen delivery. Thus cell shape, deformability, and mobility are important biomarkers which can be used to distinguish between healthy and abnormal erythrocytes.

The mechanical properties of erythrocytes play a major role in the blood flow as it is one of the most important factors that affect the flow rheology. As a result, the role of deformability in influencing erythrocyte function has been studied extensively. The stiffness of disease infected erythrocytes and its effects on the flow in microchannels were studied with recent experimental techniques [7,9]. However, experimental studies have several limitations to this topic. First, in human blood vessels, erythrocytes interact with leukocytes (white blood cells), thrombocytes (platelets), and endothelium when they are traveling in the human body. Recent experiments usually manipulate single erythrocyte or several individual cells without considering the interaction of erythrocytes with other cells. Second, it is very difficult to obtain the three-dimensional information on a flow field. Moreover, human microcirculation system has an extremely complex geometry and can hardly be manufactured in microscale.

Recent development in numerical modeling can overcome some of these problems and make reasonable predictions. Numerous studies are ongoing to qualify and identify the erythrocyte mechanics in microvascular flow [4,8,10–14]. In Ref. [8], a dissipative particle dynamics model has been developed to qualify the biophysical properties of malaria infected erythrocytes and the predictive capability of this model has

*twang@nuaa.edu.cn

†zwxing@nju.edu.cn

been demonstrated. The aggregability of erythrocytes has also been numerically simulated [11,12,14] with consideration of the mechanical properties of the cell membrane. A particle based method was used in Ref. [4] to numerically study the collective behavior of several erythrocytes in narrow capillaries for their flow induced morphology. In Ref. [14], the immersed boundary-lattice Boltzmann method was used to perform numerical simulation of erythrocyte deformation and aggregability in a stenotic arteriole. However, there is limited information on the flow behavior and erythrocyte rheological properties in complex microgeometries, such as the stenotic microchannels. There is also a critical need to develop more detailed computational simulations of cellular and molecular mechanics that accurately capture interatomic and intermolecular interactions and cytoskeletal dynamics as the cytoskeletal network is altered by the disease state [2].

Our study is motivated by recent developments in experimental investigation of individual cancer cell [15] and erythrocyte [2,16] in microfluidic devices. In this work, we investigated the traverse of individual erythrocyte through a microchannel with stenosis, which is a cardiovascular disease and is characterized by vessel wall thickening and luminal narrowing. The simulations were performed in two-dimensional flow channels. Although three-dimensional simulations have been conducted both for one and for several cells in straight tubes [4,10], two-dimensional simulations [14,17] are still helpful as a tool to aid conceptual understanding of large systems where three-dimensional simulations are extremely costly. A systematic two-dimensional study may provide insight into better understanding of the human microcirculatory system.

In this paper, a previously developed membrane model [12,18] was used to simulate the dynamics of erythrocytes, i.e., the erythrocytes were modeled as membrane particles connected by springs with stretch and compression resistance and bending rigidity. The immersed boundary method has been coupled with the fictitious domain method [19,20] to deal with the complex flow behavior in this irregular domain geometry. A series of numerical simulations were conducted to examine the complex interactions that occur between erythrocytes and constricted microvessel, such as the deformation, flow resistance, and shape transition of erythrocyte under various flow conditions. We have also studied the effect of initial positions and orientation of the cells on the motion and deformation of the erythrocytes in such vessels and compare our simulations with experimental results carried out in microfluidic devices [2,21–23]. By making qualitative and quantitative studies of several characteristic properties, such as deformation behavior, transit velocity, and shape transitions, it is hoped that one can distinguish disordered blood cells from healthy ones based on their differences in deformability using microfluidics.

II. MATHEMATICAL FORMULATION AND NUMERICAL METHODS

We considered a two-dimensional microvessel with a symmetric narrowing and employ mesoscale hydrodynamics simulations to study the rheological behavior of erythrocytes in the blood flow. The blood is assumed to be a suspension of erythrocytes in an incompressible, Newtonian fluid and the geometry of the vessel is shown in Fig. 1. The flow region is expressed as Ω_f. In order to solve the fluid flow and the fluid-cell interactions in this irregular-shaped domain, the fictitious domain method (FDM) is combined with the immersed boundary method.

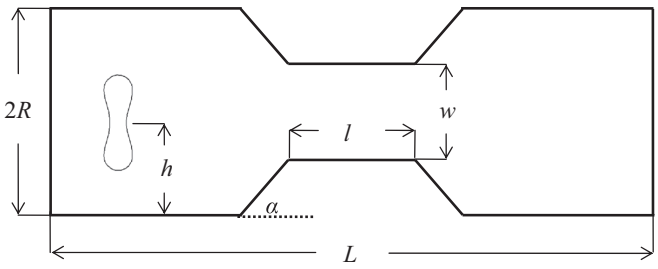

FIG. 1. Geometry of the fluid flow region Ω_f to study the deformation and motion of erythrocytes in a stenotic blood vessel where a flow is established through the channel from left to right.

A. Immersed boundary-fictitious domain scheme

The flow region we studied was not a regular-shaped domain. Thus we adopted the fictitious domain method (FDM) because in FDM the irregular-shaped domain is extended to regular shaped so that a simple structured mesh instead of unstructured mesh can be used, which substantially reduces computational complexity of the algorithm. The fictitious domain method (FDM) and its applications to fluid flow problems have been extensively described [19,20]. To employ the FDM, the flow region Ω_f is embedded in the smallest rectangular domain, which is denoted by Ω. Then the fluid flow containing erythrocytes is solved in the bigger domain Ω, and the no-flow condition in the solid region is treated as constrains. Therefore, we have the following extended Navier-Stokes equations:

$$\rho\left[\frac{\partial \mathbf{u}}{\partial t}+\mathbf{u}\cdot\nabla\mathbf{u}\right]=-\nabla p+\mu\Delta\mathbf{u}+\mathbf{f},\quad \text{in } \Omega_f, \tag{1}$$

$$\nabla\cdot\mathbf{u}=0,\quad \text{in } \Omega_f, \tag{2}$$

$$\mathbf{u}=\mathbf{0},\quad \text{in } \Omega\backslash\Omega_f, \tag{3}$$

where $\mathbf{u}(\mathbf{x},t)$ and p are the fluid velocity and pressure anywhere in the flow; ρ is the fluid density; μ is the fluid viscosity. In this paper, the fluid, i.e., the blood plasma, is assumed to be Newtonian with constant density and constant viscosity. The

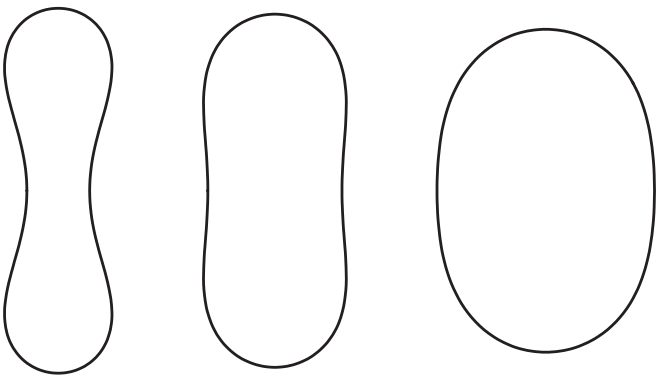

FIG. 2. From left to right: erythrocyte shapes obtained for reduced area $s^* = 0.481$, 0.7, and 0.9.

TABLE I. Parameters used for the simulations.

Parameter	Symbol	Value
Blood plasma density	ρ	1.0 g/cm^3
Blood plasma viscosity	μ	1.2, 1.5 cp
Radius of the circle in erythrocyte model	r_0	2.8 μm
Number of springs in erythrocyte model	N	76
Membrane mass in erythrocyte model	m	2.0×10^{-4} g
Friction in erythrocyte model	γ	8.8×10^{-7} Ns/m
Spring constants for erythrocyte membrane	k_l,k_b	(1.0×10^{-14})–(1.0×10^{-12}) Nm
Length of computational domain	L	85 μm
Radius of inlet (outlet)	R	9 μm
Angle between stenosis and vessel wall	α	45°
Length of stenosis	l	11 μm
Width of stenosis	w	3, 4, 5, 6, 7, 10 μm
Grid size for space	h	1/72 μm
Step size for time	Δt	1×10^{-5} ms

body force term $\mathbf{f}(\mathbf{x},t)$ is introduced to account for the force acting on the fluid-cell interface. The boundary conditions are such that, on $\partial\Omega_f$, a no-slip condition is applied and, at the inlet and outlet of the channel, a periodic flow condition is enforced. A detailed description of the solution method of Eqs. (1)–(3) can be found elsewhere [19,20].

In this study, the fluid-cell interaction was dealt with by the immersed boundary method developed by Peskin [24]. Based on this method, the boundary of the deformable object is easily calculated by the following scheme: first, the force located at the immersed boundary node $\mathbf{X} = \{X_1, X_2\}$ affects the nearby fluid mesh nodes $\mathbf{x} = \{x_1, x_2\}$ through a discrete δ function:

$$\mathbf{F}(\mathbf{x}) = \sum_{\mathbf{X}} \mathbf{F}(\mathbf{X}) D_h(\mathbf{X} - \mathbf{x}), \quad \text{for} \quad |\mathbf{X} - \mathbf{x}| \leqslant h, \tag{4}$$

where h is the uniform finite element mesh size and

$$D_h(\mathbf{X} - \mathbf{x}) = \delta_h(X_1 - x_1)\delta_h(X_2 - x_2), \tag{5}$$

with the one-dimensional (1D) discrete δ functions being

$$\delta_h(z) = \begin{cases} \frac{1}{4h}\left[1 + \cos\left(\frac{\pi z}{2h}\right)\right] & \text{for} \quad |z| \leqslant 2h, \\ 0 & \text{for} \quad |z| > 2h. \end{cases} \tag{6}$$

The force in Eq. (4) is part of the external force term of Eq. (1); next, the movement of the immersed boundary node is affected by all the nearby fluid mesh nodes through the same discrete δ function:

$$\mathbf{U}(\mathbf{X}) = \sum h^2 \mathbf{u}(\mathbf{x}) D_h(\mathbf{X} - \mathbf{x}) \quad \text{for} \quad |\mathbf{X} - \mathbf{x}| \leqslant 2h. \tag{7}$$

Finally, after each time step Δt, the position of the immersed boundary node is updated by

$$\mathbf{X}_{t+\Delta t} = \mathbf{X}_t + \Delta t \mathbf{U}(\mathbf{X}_t). \tag{8}$$

B. Erythrocyte model

Current models describe the erythrocyte as Newtonian fluid (called cytoplasm) enclosed by the cell membrane. Among these models, elastic membrane models [25,26] focus on the elastic property of the membrane and try to reproduce it through the strain energy functions. On the other hand, spring models [10,12,18,27,28] depict erythrocyte membrane with a network of springs. In this paper, we adopted the spring model introduced in Ref. [18] and modeled individual erythrocyte as cytoplasm enclosed by a membrane represented by a finite number of membrane particles connected by springs. Based

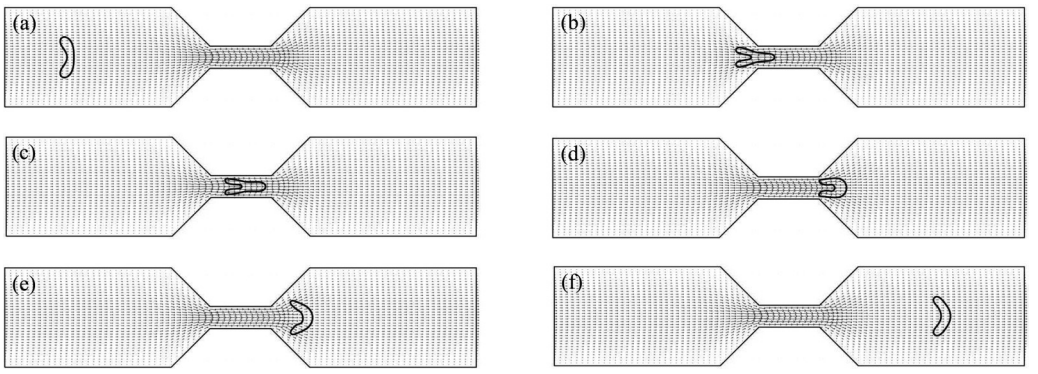

FIG. 3. Series of sequential simulation results showing the movement of a coaxial human erythrocyte through a stenotic channel, the pressure gradient across which is controlled. The time instants are (a) $t = 0.48$ ms, (b) $t = 1.90$ ms, (c) $t = 2.04$ ms, (d) $t = 2.21$ ms, (e) $t = 2.32$ ms, and (f) $t = 3.33$ ms. The erythrocyte is perpendicular to the channel axis initially. The cell moves from left to right in the flow and is forced to squeeze into a 4 μm constriction of a microchannel. After moving through the stenosis, shape recovery occurs. The spring constants for the cell membrane are $k_l = k_b = 1.0 \times 10^{-13}$ Nm.

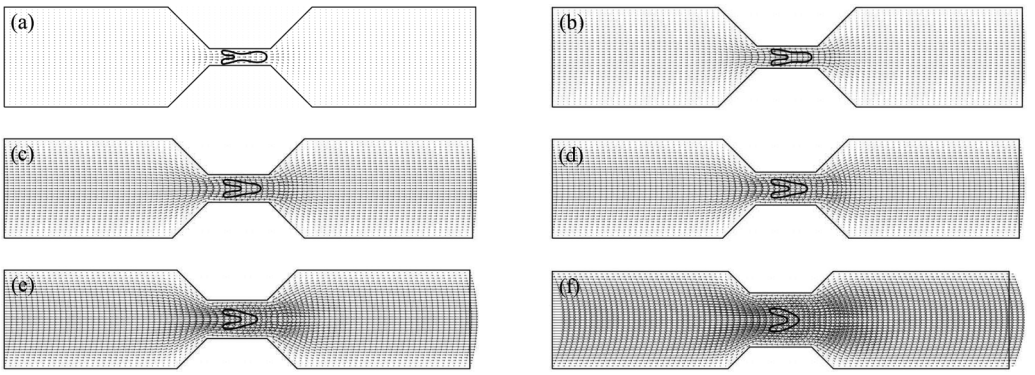

FIG. 4. Set of simulation results showing the deformed shape of an erythrocyte as it traverses the stenosis with various constriction width. (a) $w = 3\ \mu$m; $t = 5.61$ ms; (b) $w = 4\ \mu$m; $t = 2.04$ ms; (c) $w = 5\ \mu$m; $t = 1.25$ ms; (d) $w = 6\ \mu$m; $t = 1.01$ ms; (e) $w = 7\ \mu$m; $t = 0.71$ ms; (f) $w = 10\ \mu$m; $t = 3.77$ ms. The erythrocyte is perpendicular to the channel axis initially. The spring constants for the cell membrane are $k_l = k_b = 1.0 \times 10^{-13}$ Nm.

on the model, elastic energy stores in the spring due to the change of the length l of the spring with respect to its reference length l_0 and the change in angle θ between two neighboring springs. The total elastic energy of the erythrocyte membrane, $E = E_l + E_b$, is the sum of the total elastic energy for stretch and compression and the total elastic energy for bending which, in particular, are

$$E_l = \frac{k_l}{2} \sum_{i=1}^{N} \left(\frac{l_i - l_0}{l_0} \right)^2 \tag{9}$$

and

$$E_b = \frac{k_b}{2} \sum_{i=1}^{N} \tan^2(\theta_i/2). \tag{10}$$

In Eqs. (9) and (10), N is the total number of the spring elements, and k_l and k_b are spring constants for changes in length and bending angle, respectively. θ_i is the angle formed by the ith particle and its two adjoined springs [12].

The shape of the erythrocyte is obtained using the elastic spring model based on the minimum-energy principle. Initially, the cell is assumed to be a circle of radius r_0. The circle is discretized into N membrane particles so that N springs are formed by connecting the neighboring particles. Thus the reference length of the spring is then $l_0 = 2\pi r_0/N$. The shape change is stimulated by reducing the total area of the circle s_0 through a penalty function [18]:

$$\Gamma_s = \frac{k_s}{2} \left(\frac{s - s_e}{s_e} \right)^2, \tag{11}$$

where s and s_e are the time-dependent area and the equilibrium area of the erythrocyte, respectively. The total elastic spring energy E is modified as quasienergy $E_q = E + \Gamma_s$ and the force acting on the ith membrane particle now is

$$\mathbf{F}_i = -\frac{\partial E_q}{\partial \mathbf{r}_i}. \tag{12}$$

The force generated by the deformation of the membrane is treated as a part of the external force term of Eq. (1). When the area is reduced, each membrane particle moves according to the following equation of motion:

$$m\ddot{\mathbf{r}}_i + \gamma \dot{\mathbf{r}}_i = \mathbf{F}_i \tag{13}$$

Here, $\dot{(\,)}$ denotes the time derivative; m represents the membrane; γ is a friction for numerical calculation. The quasienergy decreases with the time elapse. The final shape of the erythrocyte is obtained as the quasienergy is minimized.

By taking into consideration the nonextensible property of the membrane, the values of spring constants are set as $k_l = k_b$. The value of penalty coefficient k_s is $k_b \times 10^4$. An initial circular shape is transformed into its final stable shape associated with a minimal energy for a given reduced area $s^* = s_e/s_0$ regardless of the choice of k_b. We keep track of the cell area and perimeter during the transformations. The change is less than 0.1% in the area and less than 0.5% in the perimeter for the reduced area values used in this study. It is found that the biconcave shape obtained for $s^* = 0.481$ resembles the normal physiological shape of the erythrocyte very well [12].

The bending constant is closely related to the rigidity of the membrane. A higher k_b results in a less deformable cell. Thus deformability of normal and hardened erythrocytes can be modeled by varying spring constants for these two resistances.

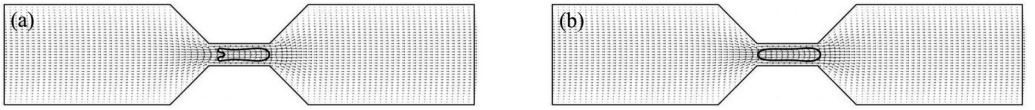

FIG. 5. Simulation results showing the effect of initial shape of the cell on the deformed shape of erythrocytes as they are at the throat of the stenosis with $w = 4\ \mu$m. (a) $s^* = 0.7$; $t = 2.03$ ms; (b) $s^* = 0.9$; $t = 2.0$ ms. The erythrocytes are perpendicular to the channel axis initially. The spring constants for the cell membrane are $k_l = k_b = 1.0 \times 10^{-13}$ Nm.

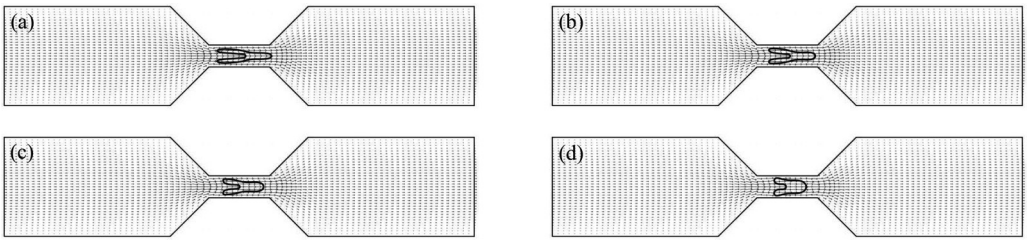

FIG. 6. Simulation results showing the effect of the membrane stiffness on the deformed shape of erythrocytes as they are at the throat of the stenosis with $w = 4$ μm. (a) $k_l = k_b = 2.5 \times 10^{-14}$ Nm, $t = 2.02$ ms; (b) $k_l = k_b = 5.0 \times 10^{-14}$ Nm, $t = 2.03$ ms; (c) $k_l = k_b = 1.0 \times 10^{-13}$ Nm, $t = 2.04$ ms; (d) $k_l = k_b = 5.0 \times 10^{-13}$ Nm, $t = 2.10$ ms. The erythrocytes are perpendicular to the channel axis initially.

III. NUMERICAL RESULTS AND DISCUSSION

We studied the hydrodynamic behavior of a single erythrocyte in a horizontal channel with a stenosis formed symmetrically at the central part of the vessel. The total length of the channel was fixed at 85 μm to ensure the full development of the flow. The grid size for the space discretization was $h = 1/72$ μm and the step size for the time was $\Delta t = 1 \times 10^{-5}$ ms for all the simulations. Other simulation parameters are listed in Table I. A constant pressure gradient was imposed at the inlet and the outlet of the channel so that a fluid flow was established from left to right. In addition, periodic boundary conditions were assumed at the left and right boundary of the domain. We performed a series of simulations to study erythrocyte deformation, flow field, and cell-structure interactions as the erythrocytes traverse the stenotic vessel.

Due to the fact that some clinical conditions are associated with shape change of erythrocytes, three shapes of erythrocytes have been chosen in the simulations, i.e., $s^* = 0.481$, 0.7, and 0.9 [12], which correspond to the shapes shown in Fig. 2. Among these, the shape with reduced area $s^* = 0.481$ is used to represent health erythrocyte and the shapes with $s^* = 0.7$ and $s^* = 0.9$ are for abnormal cells, e.g., elliptocyte and spherocyte, respectively. In particular, the length of the cell with $s^* = 0.481$ is about 7.6 μm. Moreover, two initial cell orientations, namely vertical orientation in which the erythrocyte is placed perpendicular to the channel axis and horizontal orientation in which the cell is parallel to the channel axis, are considered to study the rheological behavior of the erythrocytes in the constricted channel.

A. Stenosis induced erythrocyte deformation

Erythrocyte motions and deformations in a stenotic microvessel were analyzed in this section. The first case considered was that of a single erythrocyte of reduced area $s^* = 0.481$ moving through a stenotic channel. The vertical oriented erythrocyte was placed coaxial in the channel with a horizontal distance 2.5 μm between the cell center and the left entrance initially. Snapshots of the numerical simulations for the erythrocyte traversing a 4 μm stenosis are presented in Fig. 3. The results show that prior to entering the stenosis, the cell deforms under the hydrodynamic force. At the constriction, it further stretches into a parachute shape in order to squeeze through and the biconcave shape is recovered upon exiting the stenosis. Our model is capable of simulating erythrocyte fluidity and recovery from large deformations and good agreement with experiments [2] has been found.

To investigate the sensitivity of our results to the stenosis severity in the simulation channel, we have also performed the same simulations with constriction width $w = 3$, 5, 6, 7, and 10 μm. The results show that, for all the cases, the

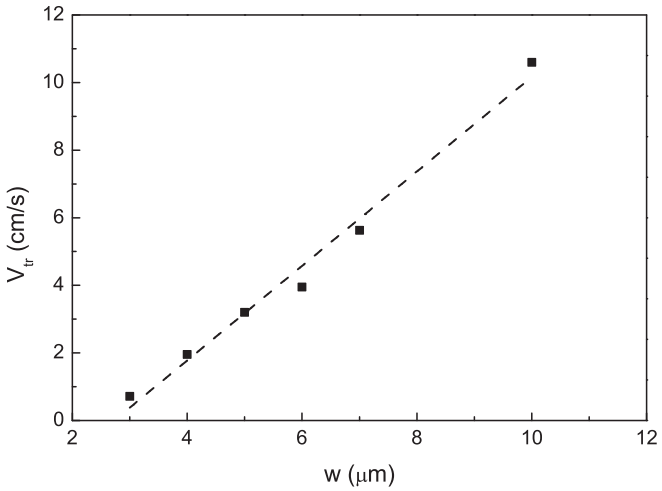

FIG. 7. Effect of stenosis severity on the transit velocities of the erythrocytes with $k_l = k_b = 1.0 \times 10^{-13}$ Nm.

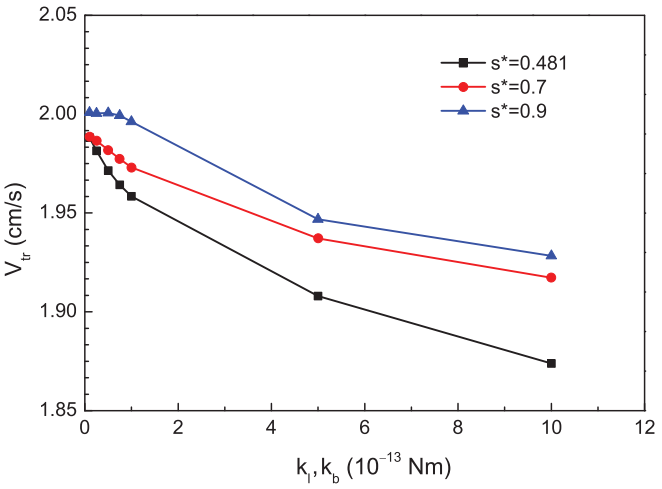

FIG. 8. (Color online) Effect of erythrocyte membrane stiffness on the average transit velocities of the cell which is perpendicular to the channel axis initially in a stenotic channel with $w = 4$ μm.

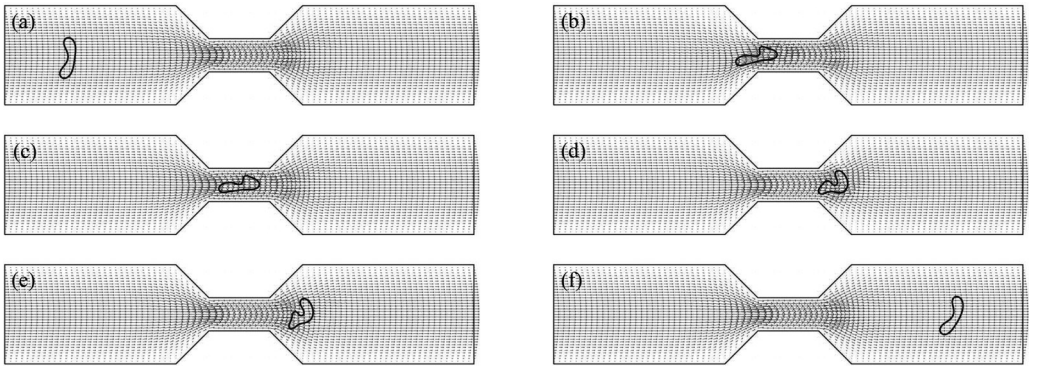

FIG. 9. Series of sequential simulation results showing the movement of a noncoaxial human erythrocyte through a stenotic channel, the pressure gradient across which is controlled. The time instants are (a) $t = 0.29$ ms, (b) $t = 0.96$ ms, (c) $t = 1.02$ ms, (d) $t = 1.12$ ms, (e) $t = 1.18$ ms, and (f) $t = 1.73$ ms. The erythrocytes are perpendicular to the channel axis initially. The cell moves from left to right into a 6 μm constriction of a microchannel. After moving through the stenosis, shape recovery occurs. The spring constants for the cell membrane are $k_l = k_b = 5.0 \times 10^{-13}$ Nm and $|R - h| = 0.5$ μm.

cell traversed the stenosis easily and deformed into parachute shapes. However, the cell is more deformed in a narrower stenosis than in a wider one. Figure 4 shows the different parachute shapes for various stenosis severities.

To study the effects of the initial shape of the cells, the next case considered was the simulation of the motions and deformations of swollen red cells in a stenotic channel. Two more cells with $s^* = 0.7$ and 0.9 were chosen to perform the same simulation. These swollen erythrocytes may be found in human blood with hereditary elliptocytosis—a congenital disorder in which the red blood cells have an elliptical or oval shape. The results of the simulation are shown in Fig. 5. For the cell with $s^* = 0.9$, the shape changes from almost ellipsoidal in static plasma to a prolonged symmetric bullet shape in the narrow part of the channel. The elongated shape will be maintained as the cell traverses the stenosis.

The deformability of the erythrocyte membrane can be significantly altered under some disease conditions. For example, the malaria infected erythrocytes could be much more rigid in comparison with healthy ones [9,29,30]. To investigate the dependence of the deformation of the cells when the cells pass through the stenosis on the membrane stiffness, we considered four characteristic values of the bending resistance while other parameters were unchanged. The cells were placed coaxial with the vessel initially. The shapes of the erythrocyte at the throat of the vessel and the velocity vectors for the fluid flow are clearly observed in Fig. 6.

B. Transit velocity

It is important to note that the transit time of erythrocytes in the microvessel depends on both the cell deformability and the friction encountered by the cell during its entry into the microchannel. Hence we define the transit velocity V_{tr} being the average velocity of the cell as it passes through the microchannel and travels a distance L. Transit velocities were calculated and analyzed in the following section for various situations encountered by the erythrocytes.

First, the effect of severity of the stenosis on the transit velocity was considered by varying the width of the throat of the vessel w for the erythrocyte with $s^* = 0.481$. Figure 7 shows a scatter plot of transit velocity against w. From the graph, it can be seen that the transit velocity increases almost linearly as the width of the stenosis increases for the parameters

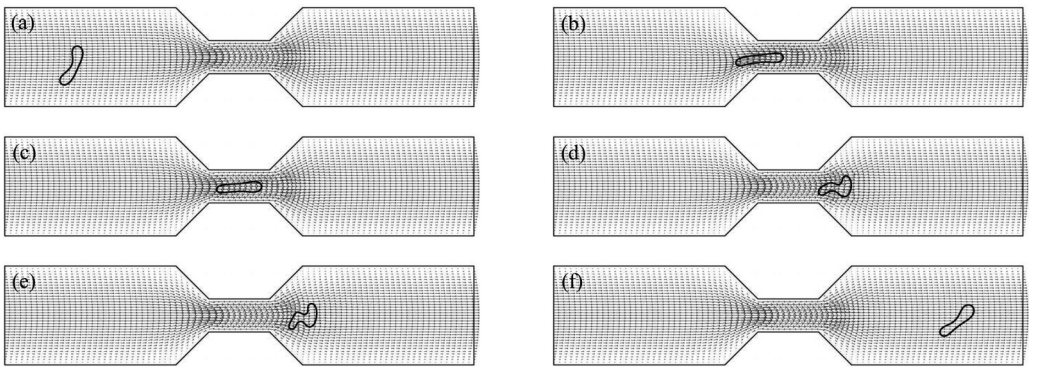

FIG. 10. Series of sequential simulation results showing the movement of a noncoaxial human erythrocyte through a stenotic channel, the pressure gradient across which was controlled. The time instants are (a) $t = 0.32$ ms, (b) $t = 0.96$ ms, (c) $t = 1.02$ ms, (d) $t = 1.12$ ms, (e) $t = 1.18$ ms, and (f) $t = 1.74$ ms. The erythrocytes are perpendicular to the channel axis initially. The cell moves from left to right into a 6 μm constriction of a microchannel. After moving through the stenosis, shape recovery occurs. The spring constants for the cell membrane are $k_l = k_b = 5.0 \times 10^{-13}$ Nm and $|R - h| = 1.5$ μm.

chosen. The reason for this behavior is that since the pressure difference at the inlet and the outlet remains the same, the flow is more blocked when the vessel is severely stenotic, which slows down the transit velocity of the cell.

Next, simulations were carried out in a vessel with 4 μm stenosis using erythrocytes of membrane constants k_l and k_b varying from 1.0×10^{-14} Nm to 1.0×10^{-12} Nm to represent the cells of various rigidity. As observed in experimental studies, the more deformable erythrocyte passes through the stenosis with large deformation. The effect of membrane stiffness on the transit velocity of erythrocytes is that the velocity deceases with the increase of the stiffness level. For instance, Fig. 8 shows the reduction of the average velocity is about 6% for the erythrocytes with $s^* = 0.481$ when the membrane constants increase from 1.0×10^{-14} Nm to 1.0×10^{-12} Nm. The reason is that more deformable cells reduce the flow resistance, thus giving rise to higher transit velocities in the stenotic part of the vessel. These results agree with the experimental observations in Ref. [9].

We also observe that for the same value of membrane constant, the transit velocities of the erythrocytes are higher for more swollen cells. This seems unusual initially as it was first thought. One possible explanation is that the cells with smaller reduced area s^* have a larger cell surface area in contact with the fluid; this will lead to increased flow resistance and may slow down the velocity of the cell.

C. Shape transitions

Thus far, calculations have been for the erythrocytes having initial coaxial positions. To further investigate the shape transition associated with the initial position of the erythrocyte, the cell was placed noncoaxial in the channel. The characteristic parameter considered was off-center distance $|R - h|$, which was defined as the distance between the cell center at initial position and the centerline of the channel.

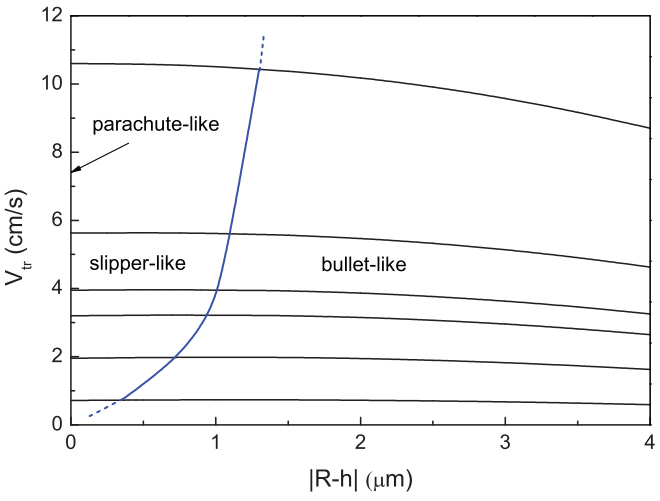

FIG. 11. (Color online) Plot showing the transit velocities of a cell traveling through the length of the microchannel as functions of off-center distance of erythrocytes for a different level of stenosis severity. The erythrocytes are perpendicular to the channel axis initially. From bottom line to top line: $w = 3, 4, 5, 6, 7$, and 10 μm. The boundary of the slipper-to-bullet transition is shown by the dark line. The spring constants for the cell membrane are $k_l = k_b = 1.0 \times 10^{-13}$ Nm.

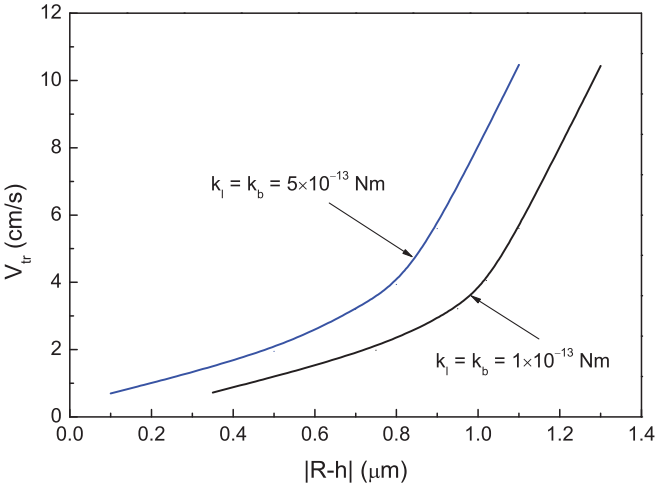

FIG. 12. (Color online) Boundaries of slipper-to-bullet transition for two different membrane constants: $k_l = k_b = 1.0 \times 10^{-13}$ Nm and $k_l = k_b = 5.0 \times 10^{-13}$ Nm.

The first case was a single erythrocyte vertically traversing the stenotic channel with off-center distance $|R - h| = 0.5$ μm. The results in Fig. 9 show that, instead of parachute shape, the cell deforms into slipperlike shape when it traverses the stenosis because the forces imposed on the cell by the flow are not symmetric. The slipper-shaped erythrocytes have been observed experimentally [22,23] and numerically [4,31]. The biconcave shape is also recovered a short distance after the cell exits the stenosis in this case.

The next case considered was that the cell was even more off center. In this case, the off-center distance was $|R - h| = 1.5$ μm so that the hydrodynamic forces imposed on the two cell tips were more different. Under this condition, the cell moves with an incline angle prior to the entrance of the stenosis. It enters the throat of the channel unfolded with bulletlike shape when it traverses the stenosis. At the distal side of the stenosis, the cell becomes slipperlike for a short period

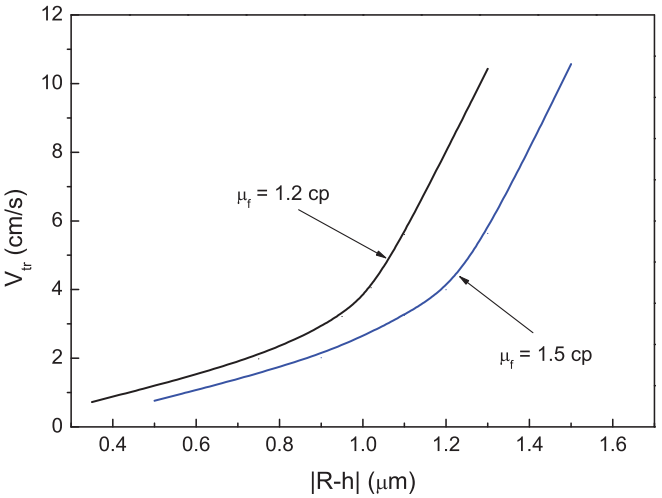

FIG. 13. (Color online) Boundaries of slipper-to-bullet transition for two different plasma viscosities: $\mu_f = 1.2$ cp and $\mu_f = 1.5$ cp.

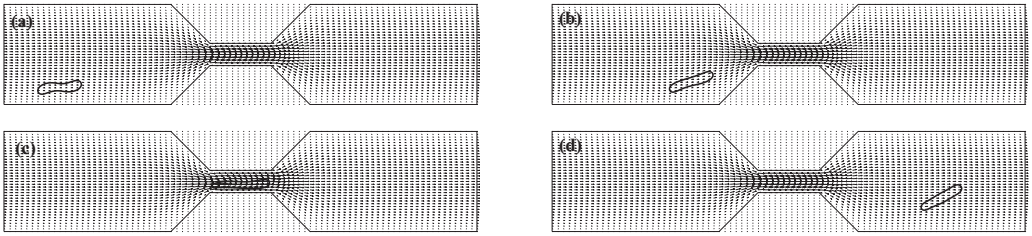

FIG. 14. Series of sequential simulation results showing the movement of a noncoaxial human erythrocyte through a stenotic channel, the pressure gradient across which is controlled. The time instants are (a) $t = 0.66$ ms, (b) $t = 2.18$ ms, (c) $t = 2.90$ ms, and (d) $t = 4.27$ ms. The erythrocyte is parallel to the channel axis initially. The cell moves from left to right into a 4 μm constriction of a microchannel. The spring constants for the cell membrane are $k_l = k_b = 1.0 \times 10^{-12}$ Nm and $|R - h| = 6$ μm.

of time, then returns to biconcave shape. The simulation results are presented in Fig. 10. The bullet-shaped erythrocytes have also been found experimentally [21].

Since symmetric shapes as parachutes only happened when the cell center coincided with the centerline of the flow, in this study we mainly investigated the transition from slipper to bullet when the cells pass through the stenosis. Figure 11 shows the transit velocity of erythrocyte for various severity of the stenosis. The transit velocity decreases with increasing level of severity. However, the effect of off-center distance on transit velocity is not significant. The width of the stenosis also affects the location of the boundary of slipper-to-bullet transition, which is also shown in Fig. 11.

We also examined how the boundary of the slipper-to-bullet transition was altered when the cells became more stiff. The cells were made less deformable by increasing membrane constants from $k_l = k_b = 1.0 \times 10^{-13}$ Nm to $k_l = k_b = 5.0 \times 10^{-13}$ Nm. The same set of stenotic microvessels, i.e., $w = 3$, 4, 5, 6, 7, and 10 μm was chosen. For clarity, only the boundaries of the transition are shown in Fig. 12. The boundary of the slipper-to-bullet transition shifts to a lower value of $|R - h|$ as k_l and k_b increase. Thus it shows that more rigid cells are more likely to become bullet shapes when passing the stenosis than more deformable cells.

Thus far, we have set the dynamic viscosity of the plasma, μ_f, to 1.2 cp. To study the effect of plasma viscosity on the shape transition, we carried out a set of simulations with $\mu_f = 1.5$ cp. The boundaries of slipper-to-bullet transitions for two different plasma viscosities are plotted in Fig. 13. The boundary for the higher viscosity case moves to bigger values of $|R - h|$.

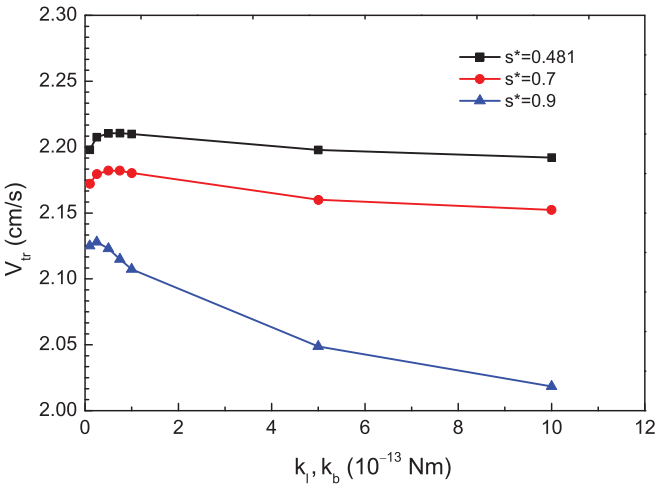

FIG. 15. (Color online) Effect of erythrocyte membrane stiffness on the average transit velocities of the cell which is parallel to the channel axis initially in a stenotic channel with $w = 4$ μm.

D. Effect of initial cell orientation

So far simulations have been done with the cells vertically located in the channel initially. In this section, we conducted the simulations of an erythrocyte traversing the same stenotic channel while the cell was initially parallel to the channel axis with a horizontal distance 3 μm between the cell center and the left entrance. Comparing to the previous simulations, different behaviors has been observed for the shape transition taking place in the stenotic channel. The erythrocytes tend to deform into bulletlike shapes at the throat of the channel, while the slipperlike shapes have not been observed for the simulation parameters chosen. Figure 14 shows the motion and deformation of an erythrocyte in a channel with a 4 μm stenosis. The reduced area for the cell is $s^* = 0.481$ and the erythrocyte was placed close to the lower boundary of the channel with an off-center distance $|R - h| = 6$ μm.

The effect of membrane stiffness on the transit velocity of erythrocytes that are parallel to the channel axis initially is that the velocity decreases with the increase of the stiffness level only for the cell with reduced area $s^* = 0.9$, while for the cells with $s^* = 0.481$ and $s^* = 0.7$, this effect is less significant. It is also shown in Fig. 15 that for the same membrane stiffness the transit velocities of the erythrocytes are higher for less swollen cells, which is an opposite dependence from the results that have been observed for the cells with vertical initial orientation.

IV. CONCLUSIONS

Computer simulations were utilized to study erythrocytes, which were characterized by mechanical modulus of the membrane. Motion and deformation of erythrocytes in a stenotic microvessel have been studied numerically by coupling the immersed boundary and fictitious domain method. We simulated with erythrocytes of various shapes and stiffness to mimic the healthy and the abnormal cells and the obtained results agree well with the experimental findings. We have also explored the dependence of the transitions from slipperlike to bulletlike shapes at the stenotic zone of the vessel on characteristic parameters such as elastic properties

of the erythrocyte membrane, initial noncoaxial positions and orientation of the cells, stenosis severities, and plasma environments.

Biconcave erythrocytes with initial vertical orientation and coaxial position were found to deform into parachute (or umbrellalike) shapes. When the cells are located off centerline initially, the cells transit to a slipperlike shape or even a bulletlike shape at the narrow part of the channel. For both parachutelike and slipperlike erythrocytes, the cells are in folded shape. The cell is symmetrically folded for the parachutelike cell and asymmetrically folded for the slipperlike cell. The asymmetry of the cells is caused by the pressure drop across the cell. The state change from slippers to bullets happens when we increase the off-center distance $|R - h|$, and the phase shift when we change the severity of the stenosis. The cells tend to deform into slipperlike shapes when the opening of the stenosis is large, while they maintain bulletlike shapes when the stenosis becomes narrow. The location of the boundary of the slipper-to-bullet transition depends on the membrane stiffness and viscosity of the blood plasma. However, for the initial horizontally oriented erythrocytes, slipperlike shape has not been observed. Moreover, simulation results show that more swollen cells travel faster if the erythrocyte cells are perpendicular to the channel axis initially provided the cells have the same rigidity, whereas opposite dependence of transit velocity on cell shape can be seen for the cells with horizontal initial orientation, i.e., more swollen cells travel slower in the stenotic channels.

The numerical method is capable of capturing the deformation and dynamics of erythrocytes in stenotic vessels and allows us to describe the complex relations among the cell mechanical properties, cell-structure interactions, and flow conditions, and to identify their effect on the rheological properties of erythrocytes in blood flow. Although the simulations were carried out at very low hematocrit, our simulation method can easily be applied to multiple cells in a blood vessel, as well as to more complex flow geometries. Furthermore, the *in silico* study of cell flow can be used in the future to address many important questions in microfluidic flows, such as flow through a bifurcated channel or changes in flow behavior in compliant blood vessels.

Studying the dynamics of erythrocytes transforming from one state to another in blood flow help us better understand several types of blood disorders, although the transition from slipper to bullet needs to be further confirmed by three-dimensional simulations. Furthermore, the modeling method presented in this paper provides us many potential applications in biology and medicine, such as blood disease diagnosis and drug delivery. Future research will be the use of this method to investigate the dependence of the flow behaviors on the channel geometry and the extension of this method to three-dimensional studies.

ACKNOWLEDGMENT

The authors acknowledge the support of National Natural Science Foundation of China (11074109).

[1] N. S. Gov and S. A. Safran, Biophys. J. **88**, 1859 (2005).
[2] J. Li, G. Lykotrafitis, M. Dao, and S. Suresh, Proc. Natl. Acad. Sci. USA **104**, 4937 (2007).
[3] H. W. G. Lim, M. Wortis, and R. Mukhopadhyay, Proc. Natl. Acad. Sci. USA **99**, 16766 (2002).
[4] J. L. McWhirter, H. Noguchi, and G. Gompper, Proc. Natl. Acad. Sci. USA **106**, 6039 (2009).
[5] M. Dao, C. T. Lim, and S. Suresh, J. Mech. Phys. Solids **51**, 2259 (2003).
[6] T. Wang and Z. W. Xing, J. Mod. Phys. **1**, 349 (2010).
[7] S. Suresh, J. Spatz, J. P. Mills, A. Micoulet, M. Dao, C. T. Lim, M. Beil, and T. Seufferlein, Acta Biomater. **1**, 15 (2005).
[8] D. A. Fedosov, B. Caswell, S. Suresh, and G. E. Karniadakis, Proc. Natl. Acad. Sci. USA **108**, 35 (2011).
[9] J. P. Shelby, J. White, K. Ganesan, P. K. Rathod, and D. T. Chiu, Proc. Natl. Acad. Sci. USA **100**, 14618 (2003).
[10] D. A. Fedosov, B. Caswell, and G. E. Karniadakis, Biophys. J. **98**, 2215 (2010).
[11] J. Zhang, P. C. Johnson, and A. S. Popel, J. Biomech. **41**, 47 (2008).
[12] T. Wang, T.-W. Pan, Z. W. Xing, and R. Glowinski, Phys. Rev. E **79**, 041916 (2009).
[13] K. I. Tsubota and S. Wada, Phys. Rev. E **81**, 011910 (2010).
[14] K. Vahidkhah and N. Fatouraee, Int. J. Numer. Meth. Biomed. Eng. **28**, 239 (2012).
[15] H. W. Hou, Q. S. Li, G. Y. H. Lee, A. P. Kumar, C. N. Ong, and C. T. Lim, Biomed. Microdevices **11**, 557 (2009).
[16] S. Braunmüller, L. Schmid, and T. Franke, J. Phys.: Condens. Matter **23**, 184116 (2011).
[17] D. A. Fedosov, J. Fornleitner, and G. Gompper, Phys. Rev. Lett. **108**, 028104 (2012).
[18] K. I. Tsubota, S. Wada, and T. Yamaguchi, J. Biomech. Sci. Eng. **1**, 159 (2006).
[19] G. Glowinski, T.-W. Pan, and J. Periaux, Comput. Methods Appl. Mech. Eng. **111**, 283 (1994).
[20] G. Glowinski, T.-W. Pan, and J. Periaux, Comput. Methods Appl. Mech. Eng. **112**, 133 (1994).
[21] H. Noguchi, G, Gompper, L. Schmid, A. Wixforth, and T. Franke, Europhys. Lett. **89**, 28002 (2010).
[22] R. Skalak, Science **164**, 717 (1969).
[23] Y. Suzuki, N. Tateishi, M. Soutani, and N. Maeda, Microcirculation **3**, 49 (1996).
[24] C. S. Peskin, J. Comput. Phys. **25**, 220 (1977).
[25] Y. Liu and W. K. Liu, J. Comput. Phys. **220**, 139 (2006).
[26] P. Bagchi, Biophys. J. **92**, 1858 (2007).
[27] H. Noguchi and G. Gompper, Proc. Natl. Acad. Sci. USA **102**, 14159 (2005).
[28] D. A. Fedosov, B. Caswell, and G. E. Karniadakis, Comput. Methods Appl. Mech. Eng. **199**, 1937 (2010).
[29] H. A. Cranston *et al.*, Science **223**, 400 (1984).
[30] C. T. Lim, J. Biomech. Sci. Eng. **1**, 82 (2006).
[31] J. L. McWhirter, H. Noguchi, and G. Gompper, Soft Matter **7**, 10967 (2011).